Applied Thermal Engineering 128 (2018) 1605–1610

Contents lists available at ScienceDirect

Applied Thermal Engineering

journal homepage: www.elsevier.com/locate/apthermeng

Research Paper

Modifying capillary pressure and boiling regime of micro-porous wicks textured with graphene oxide

Hong Seok Jo [a,1], Seongpil An [a,1], Xuan Hung Nguyen [b], Yong Il Kim [a], Boo-Hyoung Bang [a,c], Scott C. James [d], Jeehoon Choi [e,*], Sam S. Yoon [a,*]

[a] School of Mechanical Engineering, Korea University, Seoul 02841, Republic of Korea
[b] School of Engineering, Eastern International University, Binh Duong Province, Viet Nam
[c] Technology Development Team, Daewoo Inst. of Const. Tech., Suwon 16297, Republic of Korea
[d] Depts. of Geosciences and Mech. Eng., Baylor University, Waco, TX 76798, USA
[e] LG Electronics Inc., Seoul, Republic of Korea

HIGHLIGHTS

- A highly porous wicking surface was introduced to promote capillary-driven flow in a heat pipe.
- Micro-porous copper coated with graphite oxide (GO) increased the critical heat flux.
- The thin GO layer promotes hydrophilicity that enhances the wettability of the wicking surface.
- Narrowed pores due to the GO layer increase the capillary pressure and the wicking effects.

ARTICLE INFO

Article history:
Received 19 April 2017
Revised 12 September 2017
Accepted 21 September 2017
Available online 22 September 2017

Keywords:
Heat pipe
Wicking
Capillary pressure
Permeability
Boiling limitation
Graphene oxide

ABSTRACT

Liquid flow inside a heat pipe due to capillary forces can be used to cool electronic devices. To promote capillary-driven flow, a multilayer, porous wicking surface was designed for optimal liquid transport. The multilayer-porous structure consists of micro-porous structure decorated with nanomaterials. Herein, we demonstrate that micro-porous copper coated with graphene oxide (GO) has elevated capillary forces that can increase both the critical heat flux and the convective heat transfer coefficient. The thin GO layer promotes hydrophilicity that enhances the wettability of the wicking surface. However, an excessively thick GO coating can decrease permeability even in the presence of increased capillary pressures such that overall flow is hindered. In this work an optimal coating thickness is identified and characterized by heat-transfer experiments and scanning electron microscopy.

1. Introduction

The ever-growing market for faster mobile internet devices is faced with the challenge of dissipating the increased power requirements and mitigating against excessive temperature increases. A viable engineering solution to address this thermal problem is to develop a miniature cooling device using heat pipes. Moreover, there is a strong demand to increase heat fluxes in existing heat pipe designs while also allowing for continued trends toward miniaturization.

A heat pipe is a two-phase flow loop as depicted in Fig. 1a. One end of the heat pipe acts as the evaporator while the other acts as the condenser [1–6]. Its interior wall is lined with a micro-porous wick. Capillary pumping effects within the wick structure provide the driving forces for flow circulation. The maximum heat transfer rate and operational stability of heat pipes depend largely on two features: the maximum capillary pressure of the wick and the bubble nucleation regime, which govern the upper temperature limit for operation [1].

In general, capillary pumping forces increase as pore sizes decrease because the capillary pressure (ΔP) is proportional to $2\sigma/R$, where σ is the liquid's surface tension and R is the principle radius of curvature. On the one hand, decreasing the pore size or the liquid flow-path length enhances wicking effects. On the other hand, overly narrow pathways decreases permeability thereby

* Corresponding authors.
E-mail addresses: choijeehoon@gmail.com (J. Choi), skyoon@korea.ac.kr (S.S. Yoon).
[1] These authors have equally contributed.

https://doi.org/10.1016/j.applthermaleng.2017.09.103
1359-4311/

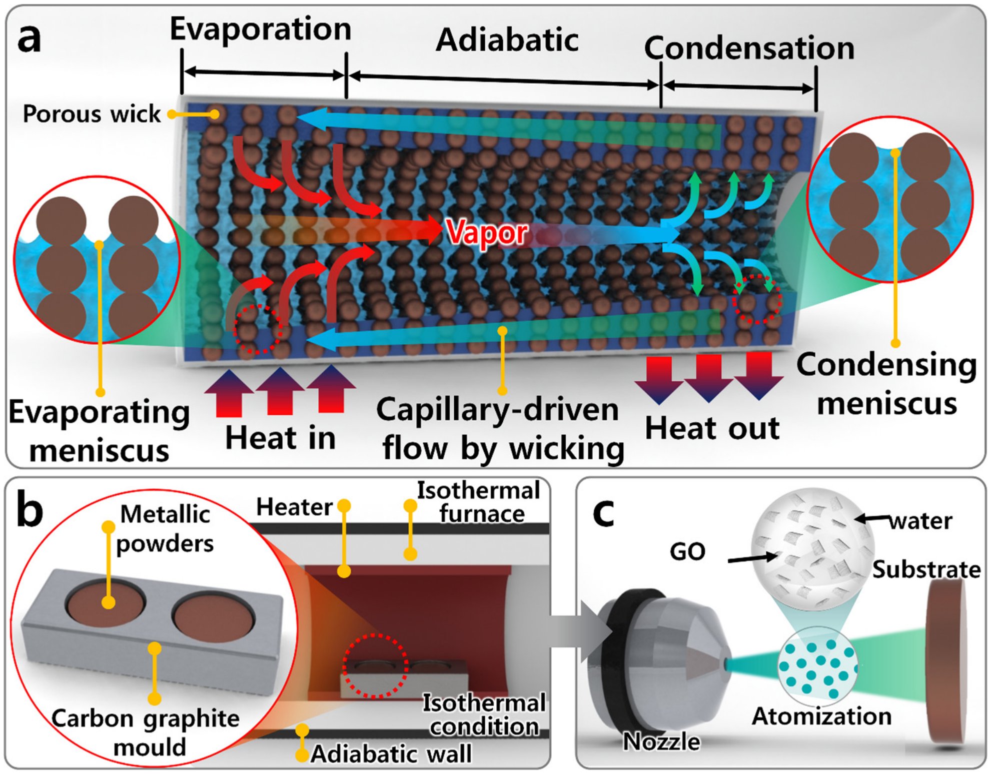

Fig. 1. Schematic of (a) the two-phase flow loop in heat pipes, (b) micro-wick sintering, and (c) GO texturing on micro wicks.

reducing the critical heat flux (CHF, the point at which film boiling occurs) or effective heat-transfer coefficient (h_{eff}). Considering these competing factors, it is important to balance capillary pressure and permeability to maximize cooling [2].

To address this challenge, academic and industrial researchers are developing enhanced multilayer, porous wicks [7–14]. Wicking is the process by which heat is dissipated through increased surface area through morphology modification. The physics of wicking are related to the available surface area, with fundamentally influences heat dissipation and hence heat-pipe performance. The focus of the current study is on how wicking effects improve heat-pipe performance, a topic notably different from others. [15,16]. The novelty of the current work lies in demonstrating the superior performance achieved through simple depositional coating. The current work surpasses previous studies because heat-pipe performance is specifically reported. The desired specifications of a miniature loop heat pipe were selected to meet the heat-dissipation requirement of 33.3 W/cm^2 [17]. Heat must be carried away to a distance of 500 mm and the chip operating temperature must stay below 70°C, which requires the wicking length scale to be only microns yielding a capillary pressure of a few kPa. Also, permeability must be in the range of 10^{-13}–10^{-14} m^2. To meet these stringent requirements, complex micro- and nanostructures have previously been used to construct a wicking system [18,19]. However, the simple GO coating developed here outperformed wicks in previous studies.

Previous studies from this group demonstrated enhanced fluid transport through a multilayer, porous wick comprising a microporous structure textured with nanomaterials. In general, nanostructures increase capillary pressures whereas microstructures afford increased permeability [19,20]. Nucleate-boiling bubbles are easily trapped in nanostructured wicks and can lead to heat-pipe failure and burnout of the electronic device being cooled [19]. It is thus critical to identify the limits of designed wicking surfaces by measuring their CHF and h_{eff} [2,19].

Copper micro-particles are used to build the micro-porous structure, which in and of itself is a wicking medium. This wicking surface is subsequently coated with graphene oxide (GO) to increase wettability [21]. This GO-textured copper wicking surface is mounted onto a heated copper plate to test pool boiling performance [22]. The role of the GO layer is to increase capillary pumping forces. However, caution must be taken not to excessively coat the micro-porous copper structure with GO, which can obstruct liquid pathways and decrease permeability. We have studied two different GO layer thicknesses (thin and thick) and tested their pool-boiling performances while quantifying their permeabilities and maximum capillary pressures.

2. Experimental design

2.1. Micro-porous wick

Non-uniform copper particles with 100–150-μm diameters (99% purity from YEI-CHANG Technology Corporation, Taiwan) were sintered at 600 °C using an isothermal furnace under a vacuum of 1 mTorr as shown in Fig. 1b. The porosities of the micro-porous wick samples were 0.5 ± 0.02 measured using Archimedes' Principle. Fabrication is described in detail elsewhere [23].

2.2. Graphene oxide nano-layers

GO was synthesized using Hummer's method [22]. The starting material was 2.5 g of 2–15-μm natural graphene flakes (Alfa Aesar, Inc.), which were immersed in an ice bath to chill below 10 °C. To these flakes were added 1 g of $NaNO_3$ and 46 ml of H_2SO_4. 6 g of $KMnO_4$ were added to the solution, which was then heated to 35 °C. After functionalization, the solution was dispersed in 92 ml of distilled water and quickly heated to 90 °C where it was held for 15 minutes. Next, 280 ml of distilled water and 40 ml of H_2O_2 were

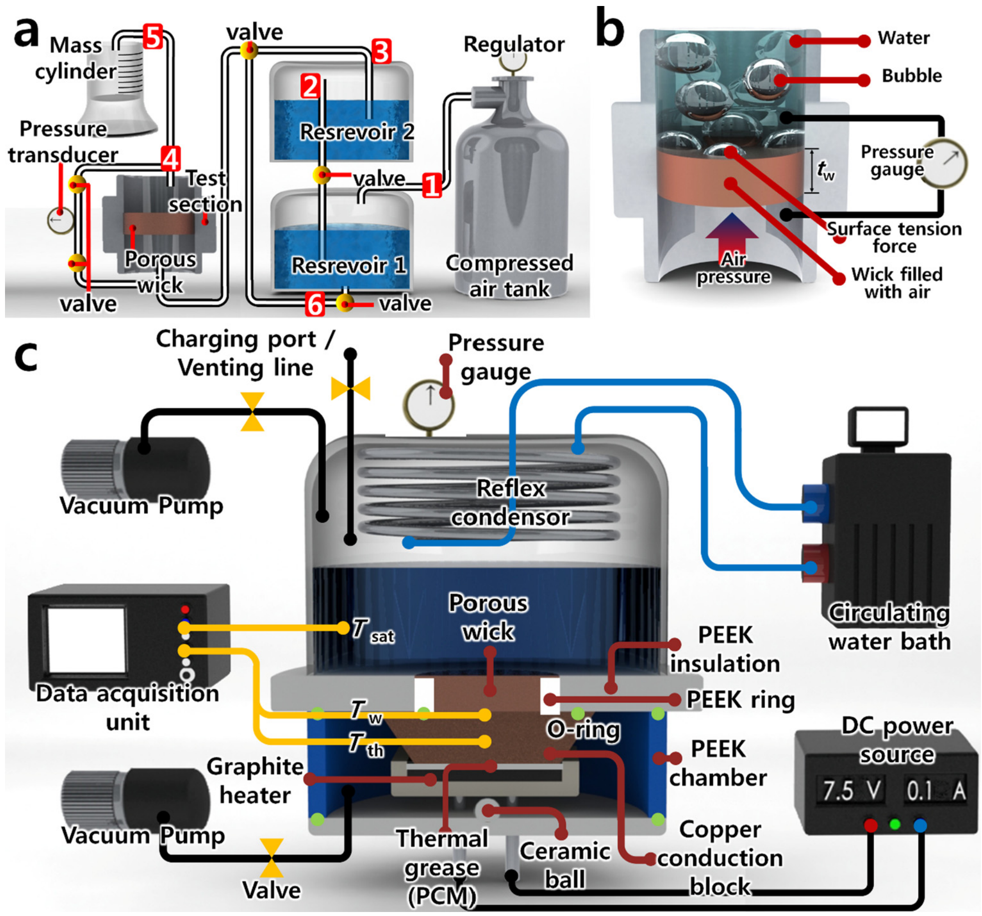

Fig. 2. Schematics of (a) permeability, (b) maximum-capillary-pressure, and (c) boiling-test apparatuses.

added to the solution. The resulting solution was washed in 21 ml of HCl solution and rinsed in ethanol. The solution was finally dried to obtain GOs at room temperature under a vacuum of 1 Torr.

Using spray deposition, GOs were textured on micro-porous wicks heated by a hot plate with layer thicknesses controlled by the amount of GO sprayed. All of the samples were fabricated as 42.0 ± 0.1–mm disks with thicknesses of 3.0 ± 0.1 mm.

GOs were suspended in DI water at a concentration of 2 mg/ml. This solution was sprayed onto copper wicks, which rested on a hot plate for water removal as shown in Fig. 1c. Different amounts (3 and 19 ml) of GO were used to coat the wick with two different (thin and thick) nano-layers.

2.3. Permeability and capillary pressure measurements

Permeability and maximum capillary pressure of wick samples were measured with the in-house-built apparatus shown in Fig. 2a and b. The apparatus is described in detail elsewhere [23]. Permeability was measured using the 1-2-3-4-5 numbered sections of the experimental apparatus as depicted in Fig. 2a. For permeability measurements, distilled water was forced through the wick sample and the pressure was then measured below and above the wick using a differential pressure transducer (Omega dyne Inc.) with an accuracy of 0.5%. Permeability was calculated using Darcy's Law [2]:

$$\kappa = \frac{\mu t_w \dot{m}}{\rho A \Delta P_w}, \tag{1}$$

where μ is the viscosity of water at room temperature, t_w is the thickness of the porous wick, ρ is the density of water, A is the cross-sectional area of the porous wick, $\dot{m}$ is the mass flow rate (measured with a mass cylinder and a stopwatch), and ΔP_w is the pressure drop across the porous wick.

Maximum capillary pressures of the wicks were measured with the bubble method [2] using the 1-6-4-5 numbered sections of the same apparatus shown in Fig. 2b. Once the wick was saturated and a column of water was established above the wick, nitrogen pressure below the wick was increased incrementally until air bubbles were observed on the top of the wick surface. Nitrogen pressure upon bubble formation was recorded as the maximum capillary pressure. In this experiment the effective radius was estimated as:

$$r_{eff} = \frac{\sigma_l \cos\theta}{P_g - \rho_l g h_l}, \tag{2}$$

where P_g is the nitrogen pressure, σ_l is water surface tension at room temperature, h_l is the height of the water column, θ is the contact angle assumed equal to 90°, and g is gravity. These experiments were performed with five samples of copper wick before and after coating to understand the effects of GO nano-coating on the permeability and maximum capillary pressure of the porous wicks.

3. Results and discussion

3.1. Nanotexturing

Photographs and scanning electron microscope (SEM) images of wicks without and with GO coating are shown in Fig. 3a and b, respectively. In Fig. 3b, GO nanotextures the microporous copper wicks. The SEM images of the copper wicks without and with GO nanotexturing look similar (middle column of Fig. 3a and b).

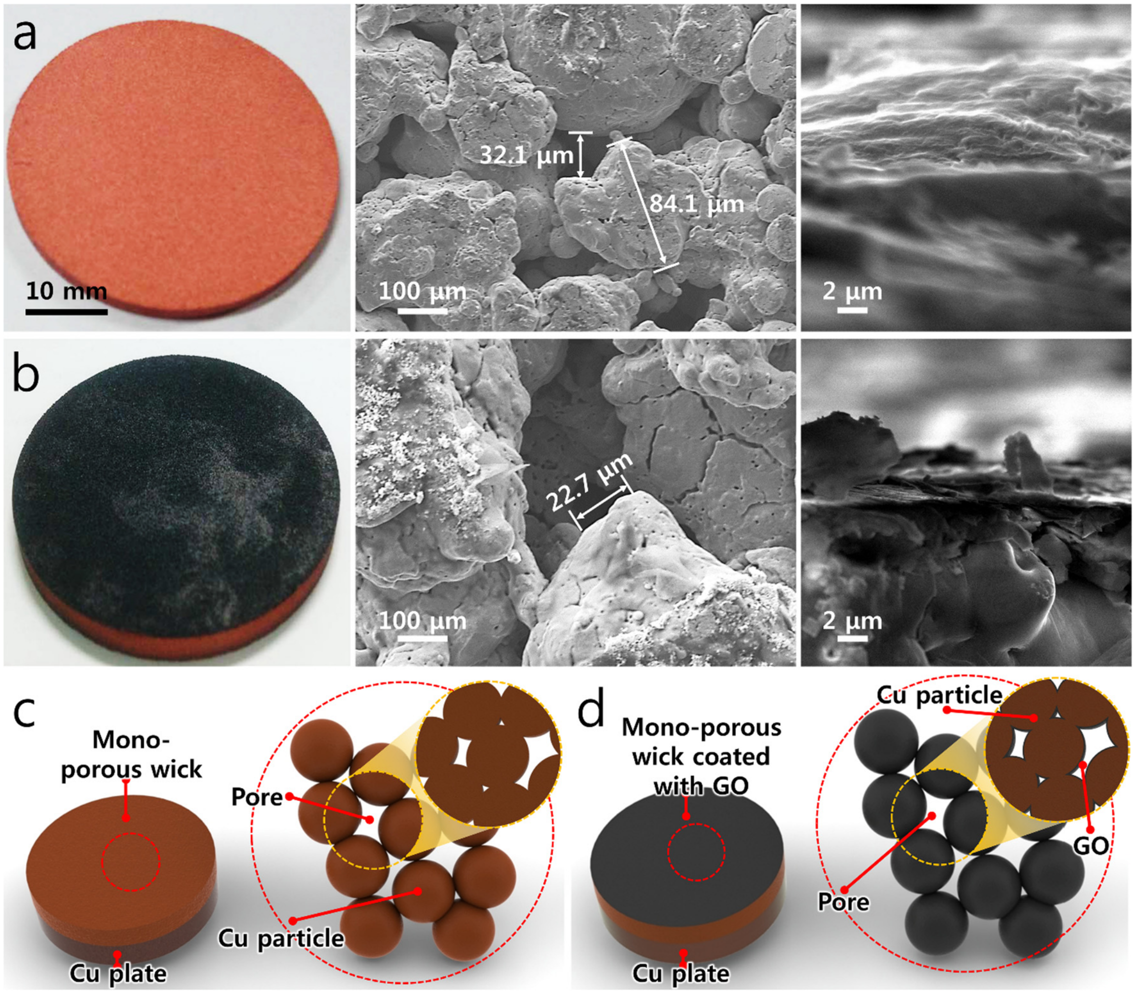

Fig. 3. (a) Porous copper wick (left: Photo, right: SEM). (b) Porous copper wick with a nano-layer of GO (first column: Photo, second column: plan SEM image, third column: cross-sectional SEM image). Schematics of (c) a porous copper wick and (d) a porous copper wick with a nano-layer of GO.

Difference between the two are evident in the cross-sectional views shown in the third column of Fig. 3 where the plate-like GO nanoparticles (5 nm in diameter and 3 nm thick) are evident. Because the GO layer on the wick surface is extremely thin, Fig. 3a and b look structurally similar. Fig. 3c and d shows the copper wick coated with GO. Pores are present between sintered copper particles through which coolant flows. When the copper wicks are coated with GO, pore sizes are reduced, which hinders flow due to narrowed channels.

3.2. Permeability and capillary pressure

The thin layer of GO coating on the porous copper wick decreases permeability and slightly increases capillary pressure through random plate overlap developed during the spray-application process. As shown in Fig. 4a, capillary pressure increased when the wick was GO nanotextured. The increase is proportional to the amount of GO solution sprayed when coating the wick surface. Conversely, Fig. 4b illustrates the decrease in wick permeability after GO coating. This decrease is also proportional to the amount of GO solution sprayed.

As shown in Fig. 4a, the maximum capillary pressure rises after GO coating. The maximum capillary pressure of the wick coated with 19 ml of GO solution increased by 23%; however, the differences between spraying 5 and 6 ml of GO solution are minor. Fig. 4b shows that wick permeability decreases as the amount of applied GO solution increases. Permeability is more sensitive to the amount of GO sprayed than is the maximum capillary pressure. Because the GO liquid can easily spread through the pore spaces inside the wick due to the hydrophilic nature of the GO coating, the contact angle between the liquid and the surface has decreased. Thus, the GO coating can enhance capillary forces through improved surface wettability. When designing heat pipes, permeability is closely associated with the operating temperature [24], thus 5 ml of GO solution optimizes our wicks through increased capillary pressure with minimal impact on permeability.

3.3. Critical heat flux and effective heat transfer coefficient

Boiling-regime testing was completed with the in-house-built apparatus shown in Fig. 2b using experimental procedure described elsewhere [15,19]. The wick samples were attached onto pure copper blocks with embedded graphene-film resistance heaters connected to a programmable DC power supply. Heat flux (q'') was controlled by changing the electric current (I) and input voltage (V). K-type sheath thermocouples with an uncertainty of 0.1% (thickness of 0.125 mm from Omega engineering) measured local temperatures at the bottom surface of sample (T_w) as well as at the copper block (T_{th}).

A highly wetting dielectric perfluorocarbon, FC-72 (3 M, Inc.), was selected as the test fluid because it is chemically inert, has good dielectric properties, and a relatively low boiling point of

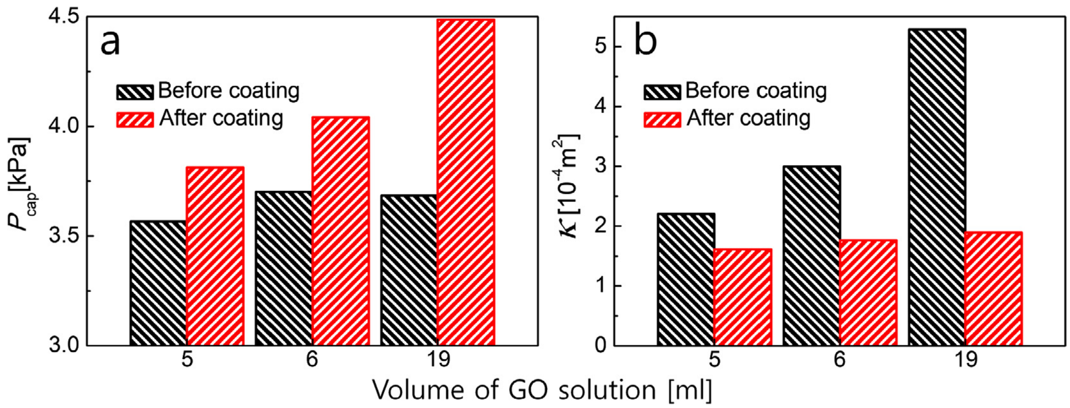

Fig. 4. Effects of GO coatings on (a) capillary pressure and (b) κ for the various GO-coated samples.

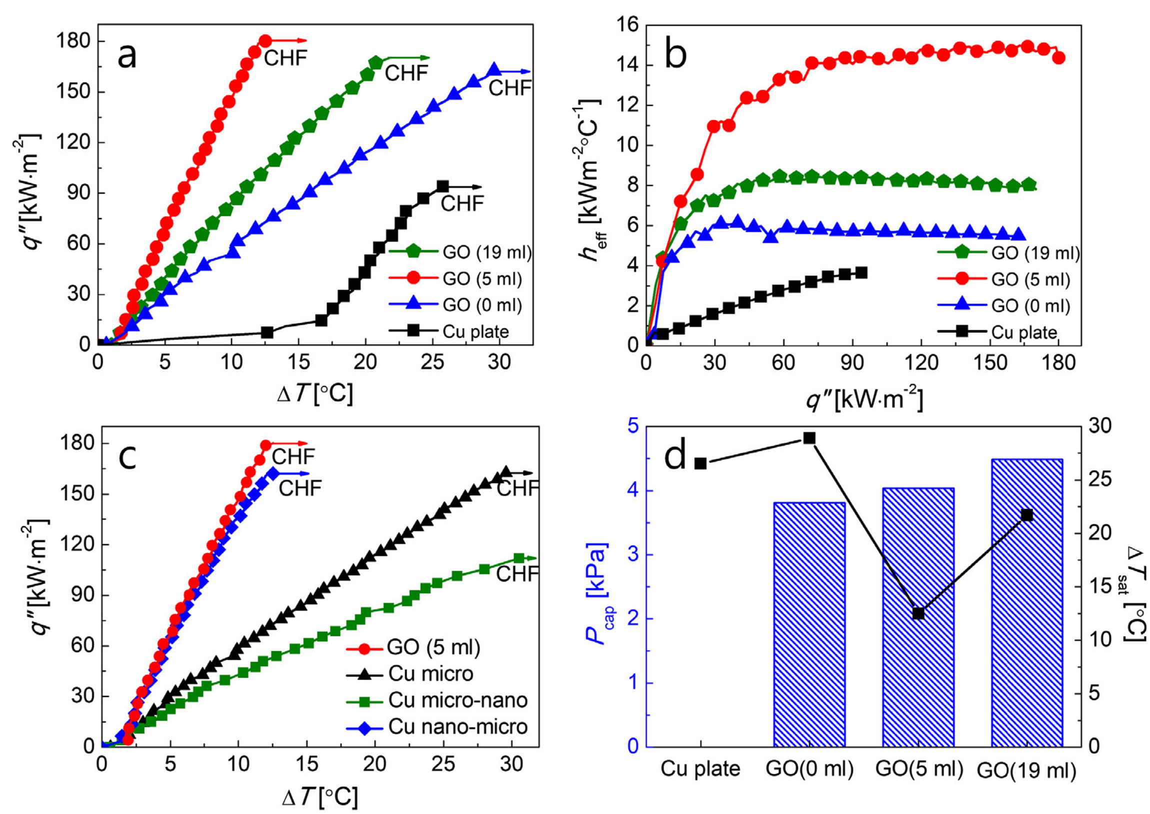

Fig. 5. (a) Boiling curves. (b) h_{eff} as a function of q'' where data correspond to (●) for Sample 1 (micro-porous wick coated with 5 ml of GO solution), (⬟) for Sample 2 (micro-porous wick coated with 19 ml of GO solution), (▲) for an uncoated micro-porous wick (0 ml of GO solution), and (■) for the polished copper plate. (c) Comparison of measured q'' to the data from Ref. [19]. (d) Capillary pressures and the ΔT_{sat} of various samples.

T_{sat} = 56 °C at 1 bar (3M Speciality Materials, Fluorinert™ Liquid FC-72, Product information, 2006). The test chamber was filled with completely degassed FC-72 to approximately 150 mm above the sample. The reflux coil condenser located at the top of the test chamber maintained a constant pressure of FC-72 throughout the test. One thermocouple was immersed in FC-72 to measure its temperature (T_{sat}). The apparatus was sealed with silicon O-rings to prevent leaks and to maintain the vacuum.

The reference resistor in the graphene film was $R = 4\ \Omega$ and it was used to determine heating power as:

$$Q = VI = I^2R. \tag{3}$$

The heat flux was calculated as:

$$q'' = \frac{Q}{A}, \tag{4}$$

The wall temperature, T_w, was obtained using T_{th} and assuming one-dimensional, steady-state heat transfer (Fig. 2c):

$$T_w = T_{th} - q''\frac{t}{k}, \tag{5}$$

where t is the spacing between the temperature measurement and the wick surface wall and k is thermal conductivity of the copper block.

The h_{eff} estimate was acquired experimentally using Newton's Law of Cooling:

$$h_{\mathrm{eff}} = \frac{q''}{\Delta T_{\mathrm{sat}}}, \tag{6}$$

where $\Delta T_{\mathrm{sat}} = T_w - T_{\mathrm{sat}}$ is the superheat.

The experimental uncertainty in heat flux was calculated through error propagation as [25]:

$$U_q = \sqrt{\left(\frac{\partial q}{\partial V}U_V\right)^2 + \left(\frac{\partial q}{\partial I}U_I\right)^2 + \left(\frac{\partial q}{\partial A}U_A\right)^2}. \tag{7}$$

The uncertainty in q'' from Eq. (7) is less than 5.3% although heat losses in the boiling test apparatus may contribute up to another 5%.

Previously, we found that maximum capillary pressure is related to the surface texture and that CHF is sensitive to this [15,16]. To investigate CHF through GO-coated wicks, three samples were studied: a mono-porous wick and multilayer, porous wicks coated with 5 or 19 ml of GO solution. As evident in Fig. 5a, GO coating increases boiling heat transfer compared to an uncoated, mono-porous wick. This is because multilayer, porous wicks coated with GO are hydrophilic and produced more bubbles than the micro-pores of the mono-porous wick; GO provides more nucleation sites. Fig. 5b compares h_{eff} across samples. Clearly, the wick alone increases heat transfer; compare the uncoated Cu plate and the wick without GO coating (0 ml). The wick coated with 5 ml of GO solution outperformed (nearly a factor of two increase in h_{eff}) the wick coated with 19 ml of GO solution. The wick coated with 5 ml of GO solution approaches optimal as it yielded the highest h_{eff} due to sufficient bubble nucleation sites with unhindered release of generated bubbles. Efficient bubble release is as important as nucleating bubbles lest vapors form an insulating layer (film boiling). Although more GO (19 ml) may yield more nucleation sites, bubble release may be inhibited due to the complex geometry of the textured layer.

Fig. 5c compares q'' (and CHF) when the Cu plate was coated with 5 ml of GO solution to values reported by Ref. [19] where bi-layer micro- and nano-scale porous composites were used. CHF was strongly dependent upon the surface morphology and the Cu nano-micro structure yielded the maximum CHF value, comparable to the optimal GO coating. However, complex micro and nano patterning requires an expensive manufacturing process involving multiple fabrication steps while GO spray deposition is simple and rapid. From an economic perspective, GO coating is clearly superior. Fig. 5d shows that capillary pressures increase with the volume of GO coating. These data reveal two important facts: First, wick alone facilitates capillary action which mobilizes liquid transport. Second, GO coating also increases the capillary pressure through textured surfaces and morphology.

Results suggest that multilayer, porous wicks coated with GO have the potential to improve upon mono-porous wicks used for heat pipes. In addition, the multilayer, porous wick coated with 5 ml of GO solution enhanced the heat-transfer performance required to meet the emerging design constraints associated with electronic devices. Efforts are underway to characterize the proposed multilayer, porous wick at higher heat loads in conventional heat pipes as well as applying them to miniaturized loop heat pipe technologies.

4. Conclusion

A sintered copper porous medium provides an efficient pathway for fluid by wicking in a heat pipe. The roughened porous structure increases the number of nucleation sites and thus increases CHF and h_{eff}. This porous medium was spray-coated with GO, which is hydrophilic (improves wettability) and increases CHF and h_{eff}. Furthermore, narrowed pores due to GO spray coating increase the capillary pressure, which enhances the wicking effects required for heat pipe operation. However, excessive GO coating decreases permeability, which degrades pool-boiling performance. Thus, the GO coating should be optimized such that it is thick enough to enhance capillary pressure (and thus wicking), but the GO is not so thick as to decrease the flow rate of the wicking coolant.

Acknowledgement

This work was supported by the National Research Council of Science & Technology (NST) grant by the Korea government (MSIP) (No. CRC-16-02-KICT), NRF-2017R1A2B4005639, NRF-2013M3A6B1078879, and NRF-2016M1A2A2936760.

References

[1] Y.F. Maydanik, Loop heat pipes, Appl. Therm. Eng. 25 (2005) 635–657.
[2] A. Faghri, Heat Pipe Science and Technology, Global Digital Press, 1995.
[3] R. Singh, A. Akbarzadeh, C. Dixon, M. Mochizuki, R.R. Riehl, Miniature loop heat pipe with flat evaporator for cooling computer CPU, IEEE Trans. Comp. Packag. Technol. 30 (2007) 42–49.
[4] V. Pastukhov, Y.F. Maydanik, Active coolers based on copper–water LHPs for desktop PC, Appl. Therm. Eng. 29 (2009) 3140–3143.
[5] X.H. Nguyen, B.H. Sung, J. Choi, S.R. Ryoo, H.S. Ko, C. Kim, Study on heat transfer performance for loop heat pipe with circular flat evaporator, Int. J. Heat Mass Transfer 55 (2012) 1304–1315.
[6] J. Choi, B. Sung, J. Yoo, C. Kim, D.-A. Borca-Tasciuc, Enhanced miniature loop heat pipe cooling system for high power density electronics, J. Therm. Sci. Eng. Appl. 4 (2012) 021008.
[7] T. Semenic, Y.-Y. Lin, I. Catton, Thermophysical properties of biporous heat pipe evaporators, J. Heat Transfer 130 (2008) 022602.
[8] C.-C. Yeh, C.-N. Chen, Y.-M. Chen, Heat transfer analysis of a loop heat pipe with biporous wicks, Int. J. Heat Mass Transfer 52 (2009) 4426–4434.
[9] Z. Liu, H. Li, B. Chen, J. Yang, W. Liu, Operational characteristics of flat type loop heat pipe with biporous wick, Int. J. Therm. Sci. 58 (2012) 180–185.
[10] J. Xu, Y. Zou, D. Yang, M. Fan, Development of biporous Ti_3AlC_2 ceramic wicks for loop heat pipe, Mater. Lett. (2013).
[11] K. Leong, C. Liu, G. Lu, Characterization of sintered copper wicks used in heat pipes, J. Porous Mater. 4 (1997) 303–308.
[12] D. Deng, D. Liang, Y. Tang, J. Peng, X. Han, M. Pan, Evaluation of capillary performance of sintered porous wicks for loop heat pipe, Exp. Therm. Fluid Sci. 50 (2013) 1–9.
[13] V. Shkolnikov, D.G. Strickland, D.P. Fenning, J.G. Santiago, Design and fabrication of porous polymer wick structures, Sens. Actuators, B 150 (2010) 556–563.
[14] L. Berti, P. Santos, E. Bazzo, R. Janssen, D. Hotza, C. Rambo, Evaluation of permeability of ceramic wick structures for two phase heat transfer devices, Appl. Therm. Eng. 31 (2011) 1076–1081.
[15] S. An, D.-Y. Kim, J.-G. Lee, H.S. Jo, M.-W. Kim, S.S. Al-Deyab, J. Choi, S.S. Yoon, Supersonically sprayed reduced graphene oxide film to enhance critical heat flux in pool boiling, Int. J. Heat Mass Transfer 98 (2016) 124–130.
[16] H.S. Jo, S. An, H.G. Park, M.-W. Kim, S.S. Al-Deyab, S.C. James, J. Choi, S.S. Yoon, Enhancement of critical heat flux and superheat through controlled wettability of cuprous-oxide fractal-like nanotextured surfaces in pool boiling, Int. J. Heat Mass Transfer 107 (2017) 105–111.
[17] T. Committee, Datacom Equipment Power Trends and Cooling Applications, ASHRAE, Atlanta, GA, 2005.
[18] J. Choi, Y. Yuan, W. Sano, D.-A. Borca-Tasciuc, Low temperature sintering of copper biporous wicks with improved maximum capillary pressure, Mater. Lett. 132 (2014) 349–352.
[19] J. Choi, B. Sung, Y. Lee, Y. Jang, H. Kang, D.-A. Borca-Tasciuc, Experimental investigation on boiling phenomena of bi-layer composite porous wicks textured with nano-porous layer, in: ASME 2014 International Mechanical Engineering Congress and Exposition, American Society of Mechanical Engineers, 2014, pp. V08BT10A057–V008BT010A057.
[20] J. Choi, Y. Yuan, D.-A. Borca-Tasciuc, H. Kang, Design, construction, and performance testing of an isothermal naphthalene heat pipe furnace, Rev. Sci. Instrum. 85 (2014) 095105.
[21] A. Buchsteiner, A. Lerf, J. Pieper, Water dynamics in graphite oxide investigated with neutron scattering, J. Phys. Chem. B 110 (2006) 22328–22338.
[22] N. Jha, P. Ramesh, E. Bekyarova, M.E. Itkis, R.C. Haddon, High energy density supercapacitor based on a hybrid carbon nanotube–reduced graphite oxide architecture, Adv. Energy Mater. 2 (2012) 438–444.
[23] J. Choi, W. Sano, W. Zhang, Y. Yuan, Y. Lee, D.-A. Borca-Tasciuc, Experimental investigation on sintered porous wicks for miniature loop heat pipe applications, Exp. Therm. Fluid Sci. 51 (2013) 271–278.
[24] J. Choi, Y. Lee, B. Sung, C. Kim, Investigation on operational characteristics of the miniature loop heat pipes with flat evaporators based on diverse vapor removal channels, in: Proceedings of 16th International Heat Pipe Conference, Lyon, France, 2012.
[25] J. Holman, Analysis of experimental data, Exp. Methods Eng. (2001) 48–143.